Contribution from the Department of Chemistry and Laboratory for Molecular Structure and Bonding, Texas A&M University, College Station, Texas 77843

Alkoxide Complexes of Niobium(III)

F. Albert Cotton,* Michael P. Diebold, and Wieslaw J. Roth

Received May 11, 1987

With $Nb_2Cl_6(THT)_3$ as starting material (THT = tetrahydrothiophene), dimeric Nb(III) alkoxide compounds can be made in good yields. These compounds, $Nb_2Cl_5(OR)(HOR)_4$ (R = Me, **1a**; R = Et, **1b**; R = *i*-Pr, **1c**), have edge-sharing bioctahedral geometries in which the metals are bridged by one chloride atom and one alkoxide ligand. Compound **1c** crystallizes in space group $P2_1/c$ with a = 9.647 (4) Å, b = 15.964 (5) Å, c = 18.286 (5) Å, β = 91.43 (3)°, V = 2815 (3) Å^3, and Z = 4. A short Nb–Nb distance and the presence of four valence d electrons are consistent with a double metal–metal bond. Compounds **1b** and **1c** are unstable in THF and with time oxidize to Nb(IV) species. These tetranuclear complexes of the type $[Nb_2OCl_4(OR)_2(THF)_2]_2$ (R = Et, **2b**; R = *i*-Pr, **2c**) form with the concomitant release of gas (e.g. ethylene in the case of **2b**). Compound **2b** crystallizes in space group $C2/c$ with a = 21.148 (5) Å, b = 12.034 (3) Å, c = 17.586 (5) Å, β = 107.53 (2)°, V = 4267 (4) Å^3, and Z = 4 (tetramers). Compound **1a** also undergoes oxidation upon storage, but in this case a different product, $Nb_2Cl_4(OMe)_4(HOMe)_2$, is isolated.

Introduction

Knowledge of Nb and Ta complexes with RO^- and ROH ligands is almost exclusively limited to those in which the metal is in its highest oxidation state.[1] Alkoxide complexes of niobium and tantalum in the +5 oxidation state have been known for over 60 years. Funk and Niederlander reported that the reaction of $TaCl_5$ with methanol or ethanol occurred with partial substitution of the chloride ions by alkoxide units, resulting in the formation of $TaCl_2(OR)_3$.[2] Since that time methods have been devised to prepare the pentaalkoxides of both niobium and tantalum from the pentachlorides.[3] Various M(V) pentaalkoxides have been studied extensively by such methods as NMR,[4] IR,[5] molecular weight determinations,[6] and X-ray crystallography.[7] In solution these compounds exist in an equilibrium between dimeric, $M_2(OR)_{10}$, and monomeric, $M(OR)_5$, forms, with the ratio of dimer to monomer depending on the R group, the solvent, and the temperature. Crystallographic analysis has shown $Nb(OMe)_5$ and $Ta(OC_6H_4CH_3)_5$ to be dimeric in the solid state.[7]

Alkoxide complexes of niobium outside of the +5 oxidation state are much less common. Several Nb(IV) alkoxide-containing complexes have been reported. Most of these are products of chemical or electrolytic reduction of $NbCl_5$ in alcohols, although a few are prepared by the reaction of alcohols with other Nb(IV) compounds. Monomeric complexes such as $NbCl_5(OR)^{2-}$ (R = Me, Et) form in solutions of high concentration of chloride ion.[8] In the presence of other potentially coordinating molecules, mixed-ligand species such as $[NbCl(OEt)_3(py)]_2$[9] and $NbCl_3(OR)bpy$[10] (R = Me, Et, *n*-Pr, *n*-Bu; py = pyridine; bpy = bipyridine) form. Complexes in the series $Nb_2(OR)_4Cl_4(HOR)_2$ (R = Me, Et, *i*-Pr) can be prepared by the reaction of the neat alcohol with $NbCl_4(THF)_2$ or $NbCl_4(CH_3CN)_2$.[11,12] Addition of an excess of OR^- to solutions of $Nb_2Cl_4(OR)_4(HOR)_2$ (R = Me, Et) gives the nonaalkoxides $Nb_2(OR)_9^-$.[13] In lower oxidation states, the complexes containing aryloxide ligands such as $Nb(OAr)_2(dmpe)_2^+$, $Nb(OAr)_2(dmpe)_2$, and $Nb(OAr)(dmpe)_2(CO)_2$ (dmpe = 1,2-bis(dimethylphosphino)ethane) have been isolated and characterized.[14]

We have recently published a preliminary report on the preparation and structure of Nb(III) complexes of formula $Nb_2Cl_5(OR)(HOR)_4$ (R = Me, Et, *i*-Pr).[15] We now wish to report the details concerning the synthesis, structure, and solution behavior of these Nb(III) compounds and the synthesis and structure of $[Nb_2OCl_4(OR)_2(THF)_2]_2$ (R = Et, *i*-Pr).

Experimental Section

All manipulations were carried out by using standard double-manifold vacuum line techniques under an atmosphere of argon. $Nb_2Cl_6(THT)_3$[16] was prepared according to the literature method. All solvents were freshly distilled from appropriate drying agents prior to use. The spectra were recorded on the following instruments: UV–visible, Cary 17d spectrometer; ^{1}H NMR, XL200 spectrometer; IR, Perkin-Elmer 783 spectrometer; GC–MS, HP 5995.

Preparation of $Nb_2Cl_5(OR)(HOR)_4$ (R = Et, 1b; R = *i*-Pr, 1c). To a solution of $Nb_2Cl_6(THT)_3$ (0.33 g; 0.5 mmol) in 15 mL of toluene is added a small amount (ca. 0.5 mL) of ROH (R = Et, *i*-Pr). After about 2 h the solution is transparent red/brown. Upon partial removal of solvent under vacuum a yellow/brown microcrystalline solid precipitates. Subsequent filtration affords **1b** and **1c** in over 60% yields. Alternatively, $Nb_2Cl_6(THT)_3$ is dissolved in neat alcohol, and after several hours solvent removal gives **1b** and **1c** in yields comparable to those above. Anal. Calcd (found) for $Nb_2Cl_5O_5C_{15}H_{31}$ (**1c**): C, 27.53 (27.87); H, 4.77 (5.78). IR (**1b**, KBr pellet; in cm^{-1}): 3195 (s, br), 2970 (m), 1615 (w, br), 1466 (w), 1438 (m), 1380 (ms), 1263 (m), 1079 (ms), 1016 (s), 903 (m), 868 (ms), 799 (m), 612 (w, br), 420 (w), 384 (w), 295 (ms). UV–vis (nm; in the neat alcohol): **1b**, 444; **1c**, 448.

Reaction of $Nb_2Cl_6(THT)_3$ with MeOH. The process is carried out as described above for ethanol and 2-propanol. However, in this case removal of solvent leads to an intractable brown oil. When the reaction is done in toluene, reddish crystals (apparently $Nb_2Cl_5(OMe)(HOMe)_4$) form within several hours, but with time these are transformed to a blue product, which has been identified as $Nb_2Cl_4(OMe)_4(HOMe)_2 \cdot 2MeOH$.[15] UV–vis (nm; **1a**, in neat MeOH): 395.

Preparation of $[Nb_2OCl_4(OR)(THF)_2]_2$ (R = Et, 2b; R = *i*-Pr, 2c). **1b** or **1c** is prepared by reaction of $Nb_2Cl_6(THT)_3$ with the neat alcohol as detailed above. The solvent is completely removed in vacuo, and the remaining solid is redissolved in 20 mL of THF. This solution is carefully layered with hexane and allowed to stand for several days. A green band appears at the solution interface but is slowly replaced by a red/black solution. During this time bubbles of gas are evolved. Single crystals of **2b** are deposited on the walls of the flask while **2c** is deposited as a microcrystalline material. Both **2b** and **2c** are virtually insoluble in THF. A sample of the gas evolved in the formation of **2b** was found by GC–MS to contain ethylene as the only organic product.

(1) Bradley, D. C.; Mehrotra, R. C.; Gaur, G. P. *Metal Alkoxides*; Academic: New York, 1978.
(2) Funk, H.; Niederlander, K. *Ber. Dtsch. Chem. Ges. B* **1929**, *62*, 1688.
(3) Bradley, D. C.; Wardlaw, W.; Witley, A. *J. Chem. Soc.* **1955**, 726.
(4) (a) Bradley, D. C.; Holloway, C. E. *J. Chem. Soc.* **1962**, 219. (b) Holloway, C. E. *J. Coord. Chem.* **1972**, *1*, 253.
(5) Bradley, D. C.; Westlake, A. H. *Proceeding of the Symposium on Coordination Chemistry*; Tihany, Hungary; Akademiai Kiado: Budapest, Hungary, 1965.
(6) Bradley, D. C.; Wardlaw, W.; Chakravarti, B. N. *J. Chem. Soc.* **1956**, 2381.
(7) (a) Reiss, J. G.; Hubert-Pfalzgraf, L. G. *Chimia* **1976**, *30*, 481. (b) Lewis, L. N.; Garbauskas, M. F. *Inorg. Chem.* **1985**, *24*, 383.
(8) Wentworth, R. A. D.; Brubaker, C. H., Jr. *Inorg. Chem.* **1963**, *2*, 551.
(9) Wentworth, R. A. D.; Brubaker, C. H., Jr. *Inorg. Chem.* **1964**, *3*, 47.
(10) Vuletic, N.; Djordjevic, C. *J. Chem. Soc., Dalton Trans.* **1973**, 550.
(11) Cotton, F. A.; Diebold, M. P.; Roth, W. J. *Inorg. Chem.*, preceding paper in this issue.
(12) Gut, R.; Perron, W. *J. Less-Common Met.* **1972**, *26*, 369.
(13) Cotton, F. A.; Diebold, M. P.; Roth, W. J., manuscript in preparation.
(14) Coffindaffer, T. W.; Rothwell, I. P.; Folting, K.; Huffman, J. C.; Streib, W. E. *J. Chem. Soc., Chem. Commun.* **1985**, 1519.
(15) Cotton, F. A.; Diebold, M. P.; Roth, W. J. *Inorg. Chem.* **1985**, *24*, 3509.
(16) (a) Maas, E. T., Jr.; McCarley, R. E. *Inorg. Chem.* **1973**, *12*, 1096. (b) Templeton, J. L.; McCarley, R. E. *Inorg. Chem.* **1978**, *17*, 2293.

0020-1669/87/1326-3323$01.50/0 © 1987 American Chemical Society

Table I. Crystallographic Data for **1c** and **2b**

formula	$Nb_2Cl_5O_5C_{15}H_{39}$	$Nb_2Cl_4O_5C_{12}H_{26}$
fw	662.55	577.96
space group	$P2_1/n$	$C2/c$
systematic absences	$0k0$, $k \neq 2n$; $h0l$, $h + l \neq 2n$	hkl, $h + k \neq 2n$; $h0l$, $l \neq 2n$
a, Å	9.647 (4)	21.148 (5)
b, Å	15.964 (5)	12.034 (3)
c, Å	18.286 (5)	17.586 (5)
α, deg	90.0	90.0
β, deg	91.43 (3)	107.53 (2)
γ, deg	90.0	90.0
V, Å^3	2815 (3)	4267 (4)
Z	4	8
d_{calcd}, g/cm^3	1.563	1.799
cryst size, mm	0.3 × 0.3 × 0.2	0.2 × 0.2 × 0.15
μ(Mo, Kα), cm^{-1}	12.783	15.507
data collecn instrument	Enraf-Nonius CAD-4	Syntex P$\bar{1}$
radiation (monochromated in incident beam)	Mo Kα ($\lambda_{\bar{a}}$ = 0.710 73 Å)	
orientation rflns: no.; range (2θ), deg	25; 12.0–27.0	15; 16.1–28.4
temp, °C	21	5
scan method	ω–2θ	ω–2θ
data collecn range, 2θ, deg	$4 < 2\theta < 45$	$4 < 2\theta < 50$
no. of unique data, total with $F_o^2 > 3\sigma(F_o^2)$	2167, 955	1793, 1529
no. of params refined	144	168
R^a	0.0641	0.0476
R_w^b	0.0713	0.0624
quality-of-fit indicator^c	1.495	1.251
largest shift/esd, final cycle	0.01	0.05
largest peak, e/Å^3	0.883	0.681

$^a R = \sum||F_o| - |F_c||/\sum|F_o|$. $^b R_w = [\sum w(|F_o| - |F_c|)^2/\sum w|F_o|^2]^{1/2}$; $w = 1/\sigma^2(|F_o|)$. ^{c}Quality of fit = $[\sum w(|F_o| - |F_c|)^2/(N_{observns} - N_{params})]^{1/2}$.

X-ray Crystallography. X-ray structure determinations of compounds **1c** and **2b** were carried out by the following data collection and structure refinement procedures, which are routine to this laboratory and have been described elsewhere in detail.[17,18] Lorentz and polarization corrections were applied to all data, and for compound **1c** an empirical absorption correction based on azimuthal (ψ) scans of eight reflections with Eulerian angle χ near 90° was made. The relevant crystallographic parameters for **1c** and **2b** are summarized in Table I.

In each case the positions of the niobium atoms were derived from a three-dimensional Patterson function. The remainder of the non-hydrogen atoms were determined by an alternating series of least-squares refinements and difference Fourier syntheses. In **2b** a disorder was present in both the terminal ethoxide ligand and one of the THF molecules. For the methyl carbon atom on the terminal ethoxide, two peaks giving reasonable distances and angles were present in the difference Fourier map. Both were included and given equal occupancies. Likewise, two orientations, related by a rotation about the M–O vector, were seen for one of the THF rings. Each orientation was given an occupancy factor of $^1/_2$. For both structures selected atoms were given anisotropic displacement parameters (see Tables II and III) and the molecules were refined to convergence. In neither case could hydrogen atoms be located in the final difference Fourier map, and no attempt was made to include them in calculated positions.

Tables of observed and calculated structure factors and anisotropic equivalent displacement parameters for both compounds are available as supplementary material.

Results and Discussion

Molecular Structures. The positional and isotropic-equivalent displacement parameters for **1c** and **2b** are given in Tables II and III, respectively. Important bond distances and angles for **1c** are presented in Table IV and those for **2b** in Table V. Complete listings of interatomic dimensions for both compounds are included as supplementary material.

Compound **1c** exists as discrete, dinuclear molecules. The dimer, shown in Figure 1, has an edge-sharing bioctahedral geometry. The short Nb–Nb distance is consistent with a double metal–metal bond, and this geometry is in fact quite common for compounds of niobium and tantalum containing double M–M bonds. While most known edge-sharing bioctahedral complexes

Table II. Positional and Isotropic-Equivalent Displacement Parameters for Nb_2Cl_5(O-*i*-Pr)(HO-*i*-Pr)$_4$ (**1c**)^a

atom	x	y	z	B, Å^2
Nb(1)	−0.2878 (3)	−0.2236 (2)	0.1581 (1)	2.14 (6)
Nb(2)	−0.2427 (3)	−0.2185 (2)	0.0179 (1)	1.94 (6)
Cl(1)	−0.282 (1)	−0.0899 (4)	0.0891 (5)	2.9 (2)
Cl(2)	−0.5397 (9)	−0.2266 (7)	0.1448 (5)	4.2 (2)
Cl(3)	−0.297 (1)	−0.3329 (5)	0.2565 (5)	4.2 (2)
Cl(4)	0.0075 (9)	−0.2003 (6)	0.0307 (4)	3.6 (2)
Cl(5)	−0.219 (1)	−0.3190 (5)	−0.0844 (5)	3.9 (2)
O(1)	−0.248 (2)	−0.318 (1)	0.086 (1)	2.1 (4)*
O(2)	−0.077 (2)	−0.206 (1)	0.183 (1)	2.8 (5)*
O(3)	−0.317 (2)	−0.136 (1)	0.251 (1)	2.6 (5)*
O(4)	−0.460 (2)	−0.216 (1)	−0.006 (1)	2.9 (4)*
O(5)	−0.230 (2)	−0.125 (1)	−0.075 (1)	2.2 (4)*
C(10)	−0.223 (3)	−0.415 (2)	0.091 (2)	3.6 (8)*
C(11)	−0.353 (5)	−0.443 (3)	0.052 (3)	9 (1)*
C(12)	−0.093 (4)	−0.436 (2)	0.067 (2)	6 (1)*
C(20)	0.008 (3)	−0.215 (2)	0.251 (2)	2.6 (6)*
C(21)	0.111 (4)	−0.289 (2)	0.242 (2)	4.4 (8)*
C(22)	0.071 (4)	−0.133 (2)	0.271 (2)	7 (1)*
C(30)	−0.391 (4)	−0.054 (2)	0.254 (2)	3.6 (8)*
C(31)	−0.514 (4)	−0.068 (2)	0.302 (2)	6 (1)*
C(32)	−0.276 (5)	0.006 (3)	0.280 (3)	9 (1)*
C(40)	−0.545 (4)	−0.224 (2)	−0.077 (2)	4.8 (8)*
C(41)	−0.674 (5)	−0.291 (3)	−0.056 (2)	8 (1)*
C(42)	−0.618 (4)	−0.138 (2)	−0.088 (2)	5 (1)*
C(50)	−0.163 (3)	−0.037 (2)	−0.076 (2)	3.8 (9)*
C(51)	−0.271 (4)	0.021 (3)	−0.102 (2)	7 (1)*
C(52)	−0.048 (4)	−0.046 (2)	−0.126 (2)	6 (1)*

^{a}Starred values indicate atoms refined isotropically. Anisotropically refined atoms are given in the form of the isotropic-equivalent thermal parameter, defined as $^4/_3[a^2\beta_{11} + b^2\beta_{22} + c^2\beta_{33} + ab(\cos\gamma)\beta_{12} + ac(\cos\beta)\beta_{13} + bc(\cos\alpha)\beta_{23}]$.

Table III. Positional and Isotropic-Equivalent Displacement Parameters for $[Nb_2OCl_4(OEt)_2(THF)_2]_2$ (**2b**)^a

atom	x	y	z	B, Å^2
Nb(1)	−0.10995 (5)	−0.0350 (1)	0.01654 (7)	4.32 (3)
Nb(2)	−0.03906 (5)	0.17233 (9)	0.02554 (6)	4.10 (2)
Cl(1)	−0.0273 (2)	0.0393 (3)	0.1379 (2)	5.20 (8)
Cl(2)	−0.1858 (2)	−0.1330 (3)	−0.0943 (2)	7.5 (1)
Cl(3)	−0.1190 (2)	0.2735 (3)	0.0738 (2)	7.2 (1)
Cl(4)	−0.0471 (2)	0.3186 (3)	−0.0716 (2)	7.7 (1)
O(1)	−0.1084 (4)	0.0885 (7)	−0.0605 (4)	4.8 (2)
O(2)	−0.1761 (4)	0.0183 (8)	0.0501 (5)	6.8 (2)
O(3)	−0.1096 (4)	−0.1868 (7)	0.0895 (5)	5.7 (2)
O(4)	0.0330 (4)	0.2782 (6)	0.1146 (5)	5.2 (2)
O(5)	−0.0329 (4)	−0.1090 (6)	−0.0071 (4)	4.9 (2)
C(11)	−0.1394 (7)	0.108 (1)	−0.1480 (8)	7.0 (4)*
C(12)	−0.2048 (9)	0.164 (2)	−0.153 (1)	10.7 (6)*
C(21)	−0.235 (1)	0.062 (2)	0.070 (1)	11.2 (6)*
C(22)	−0.216 (2)	0.045 (3)	0.151 (2)	9 (1)*
C(22A)	−0.268 (2)	0.005 (3)	0.107 (2)	9.0 (9)*
C(31)	−0.134 (1)	−0.301 (2)	0.049 (1)	5.5 (6)*
C(32)	−0.115 (1)	−0.375 (2)	0.116 (1)	5.8 (6)*
C(33)	−0.131 (1)	−0.298 (2)	0.187 (1)	5.8 (6)*
C(34)	−0.105 (1)	−0.182 (3)	0.172 (2)	7.8 (8)*
C(31A)	−0.060 (1)	−0.209 (2)	0.170 (1)	6.0 (6)*
C(32A)	−0.079 (2)	−0.330 (3)	0.182 (2)	8.8 (9)*
C(33A)	−0.136 (2)	−0.355 (3)	0.145 (2)	9 (1)*
C(34A)	−0.161 (2)	−0.265 (3)	0.075 (2)	7.9 (8)*
C(41)	0.0718 (8)	0.237 (2)	0.1921 (9)	9.0 (5)*
C(42)	0.1254 (9)	0.336 (2)	0.221 (1)	10.6 (5)*
C(43)	0.0835 (8)	0.429 (2)	0.193 (1)	9.5 (5)*
C(44)	0.0401 (9)	0.398 (2)	0.109 (1)	10.2 (5)*

^{a}See footnote *a* of Table II.

(17) Crystal structure determinations were carried out by standard methods that have been detailed previously: (a) Bino, A.; Cotton, F. A.; Fanwick, P. E. *Inorg. Chem.* **1979**, *18*, 3558. (b) Cotton, F. A.; Frenz, B. A.; Deganello, G.; Shaver, A. *J. Organomet. Chem.* **1973**, *50*, 227.

(18) Calculations were made on the VAX-11/780 computer at the Department of Chemistry, Texas A&M University, College Station, TX, with the VAX-SDP software package.

Table IV. Important Bond Distances (Å) and Angles (deg) in $Nb_2Cl_5(O\text{-}i\text{-}Pr)(HO\text{-}i\text{-}Pr)_4$[a]

Nb(1)–Nb(2)	2.611 (3)	Nb(2)–Cl(1)	2.465 (8)
Nb(1)–Cl(1)	2.480 (9)	Nb(2)–Cl(4)	2.436 (9)
Nb(1)–Cl(2)	2.437 (9)	Nb(2)–Cl(5)	2.480 (10)
Nb(1)–Cl(3)	2.509 (9)	Nb(2)–O(1)	2.02 (2)
Nb(1)–O(1)	2.03 (2)	Nb(2)–O(4)	2.13 (2)
Nb(1)–O(2)	2.09 (2)	Nb(2)–O(5)	2.27 (2)
Nb(1)–O(3)	2.22 (2)		
Nb(2)–Nb(1)–Cl(1)	57.8 (2)	Nb(1)–Nb(2)–O(4)	91.0 (5)
Nb(2)–Nb(1)–Cl(2)	95.4 (2)	Nb(1)–Nb(2)–O(5)	140.2 (5)
Nb(2)–Nb(1)–Cl(3)	137.3 (3)	Cl(1)–Nb(2)–Cl(4)	90.9 (4)
Nb(2)–Nb(1)–O(1)	49.7 (5)	Cl(1)–Nb(2)–Cl(5)	162.8 (4)
Nb(2)–Nb(1)–O(2)	91.3 (5)	Cl(1)–Nb(2)–O(1)	108.5 (6)
Nb(2)–Nb(1)–O(3)	139.1 (5)	Cl(1)–Nb(2)–O(4)	85.8 (6)
Cl(1)–Nb(1)–Cl(2)	90.0 (4)	Cl(1)–Nb(2)–O(5)	81.8 (5)
Cl(1)–Nb(1)–Cl(3)	164.7 (3)	Cl(4)–Nb(2)–Cl(5)	92.4 (4)
Cl(1)–Nb(1)–O(1)	107.5 (6)	Cl(4)–Nb(2)–O(1)	94.4 (7)
Cl(1)–Nb(1)–O(2)	87.9 (6)	Cl(4)–Nb(2)–O(4)	169.6 (6)
Cl(1)–Nb(1)–O(3)	81.3 (5)	Cl(4)–Nb(2)–O(5)	85.5 (7)
Cl(2)–Nb(1)–Cl(3)	90.3 (4)	Cl(5)–Nb(2)–O(1)	88.0 (6)
Cl(2)–Nb(1)–O(1)	97.1 (7)	Cl(5)–Nb(2)–O(4)	88.0 (6)
Cl(2)–Nb(1)–O(2)	170.5 (6)	Cl(5)–Nb(2)–O(5)	81.6 (5)
Cl(2)–Nb(1)–O(3)	86.7 (6)	O(1)–Nb(2)–O(4)	96.0 (8)
Cl(3)–Nb(1)–O(1)	87.6 (6)	O(1)–Nb(2)–O(5)	169.6 (8)
Cl(3)–Nb(1)–O(2)	89.3 (6)	O(4)–Nb(2)–O(5)	84.3 (8)
Cl(3)–Nb(1)–O(3)	83.4 (5)	Nb(1)–Cl(1)–Nb(2)	63.7 (2)
O(1)–Nb(1)–O(2)	92.4 (8)	Nb(1)–O(1)–Nb(2)	80.2 (6)
O(1)–Nb(1)–O(3)	170.3 (8)	Nb(1)–O(1)–C(10)	136 (2)
O(2)–Nb(1)–O(3)	83.8 (8)	Nb(2)–O(1)–C(10)	143 (2)
Nb(1)–Nb(2)–Cl(1)	58.4 (2)	Nb(1)–O(2)–C(20)	133 (2)
Nb(1)–Nb(2)–Cl(4)	95.7 (2)	Nb(1)–O(3)–C(30)	130 (2)
Nb(1)–Nb(2)–Cl(5)	137.8 (3)	Nb(2)–O(4)–C(40)	133 (2)
Nb(1)–Nb(2)–O(1)	50.2 (5)	Nb(2)–O(5)–C(50)	130 (2)

[a] Numbers in parentheses are estimated standard deviations in the least significant digits.

Table V. Important Bond Distances (Å) and Angles (deg) in $[Nb_2OCl_4(OEt)_2(THF)_2]_2$[a]

Nb(1)–Nb(2)	2.891 (1)	Nb(1)–O(5)	2.008 (7)
Nb(1)–Nb(2)′	3.823 (1)	Nb(2)–Cl(1)	2.497 (3)
Nb(1)–Cl(1)	2.482 (3)	Nb(2)–Cl(3)	2.435 (3)
Nb(1)–Cl(2)	2.424 (3)	Nb(2)–Cl(4)	2.423 (3)
Nb(1)–O(1)	2.018 (7)	Nb(2)–O(1)	2.031 (7)
Nb(1)–O(2)	1.794 (8)	Nb(2)–O(4)	2.227 (7)
Nb(1)–O(3)	2.231 (8)	Nb(2)–O(5)	1.816 (7)
Cl(1)–Nb(1)–Cl(2)	172.0 (1)	Cl(1)–Nb(2)–O(4)	85.8 (2)
Cl(1)–Nb(1)–O(1)	99.4 (2)	Cl(1)–Nb(2)–O(5)	89.1 (2)
Cl(1)–Nb(1)–O(2)	90.3 (3)	Cl(3)–Nb(2)–Cl(4)	88.5 (1)
Cl(1)–Nb(1)–O(3)	85.5 (2)	Cl(3)–Nb(2)–O(1)	95.0 (2)
Cl(1)–Nb(1)–O(5)	86.1 (2)	Cl(3)–Nb(2)–O(4)	82.4 (2)
Cl(2)–Nb(1)–O(1)	87.6 (2)	Cl(3)–Nb(2)–O(5)	168.4 (3)
Cl(2)–Nb(1)–O(2)	92.6 (3)	Cl(4)–Nb(2)–O(1)	87.3 (2)
Cl(2)–Nb(1)–O(3)	87.2 (2)	Cl(4)–Nb(2)–O(4)	88.2 (2)
Cl(2)–Nb(1)–O(5)	90.0 (2)	Cl(4)–Nb(2)–O(5)	93.6 (3)
O(1)–Nb(1)–O(2)	97.5 (4)	O(1)–Nb(2)–O(4)	174.9 (3)
O(1)–Nb(1)–O(3)	172.4 (3)	O(1)–Nb(2)–O(5)	96.6 (3)
O(1)–Nb(1)–O(5)	90.6 (3)	O(4)–Nb(2)–O(5)	86.2 (3)
O(2)–Nb(1)–O(3)	88.3 (4)	Nb(1)–Cl(1)–Nb(2)	70.98 (8)
O(2)–Nb(1)–O(5)	171.7 (4)	Nb(1)–O(1)–Nb(2)	91.1 (3)
O(3)–Nb(1)–O(5)	83.9 (3)	Nb(1)–O(1)–C(11)	135.4 (7)
Cl(1)–Nb(2)–Cl(3)	87.6 (1)	Nb(2)–O(1)–C(11)	133.2 (7)
Cl(1)–Nb(2)–Cl(4)	173.2 (1)	Nb(1)–O(2)–C(21)	175 (1)
Cl(1)–Nb(2)–O(1)	98.6 (2)	Nb(1)–O(5)–Nb(2)	177.7 (4)

[a] Numbers in parentheses are estimated standard deviations in the least significant digits.

of Nb and Ta are bridged by equivalent ligands, in this case two different atoms bridge the metal atoms. One is the oxygen atom of a propoxide anion, and the other is a chlorine atom. On each metal a chlorine atom is trans to the bridging chlorine atom and propanol molecules are trans to the bridging propoxide ligand. One axial position on each metal atom is occupied by a chlorine atom and the other by a propanol group, and these are arranged such that there is a virtual C_2 axis coincident with the vector joining

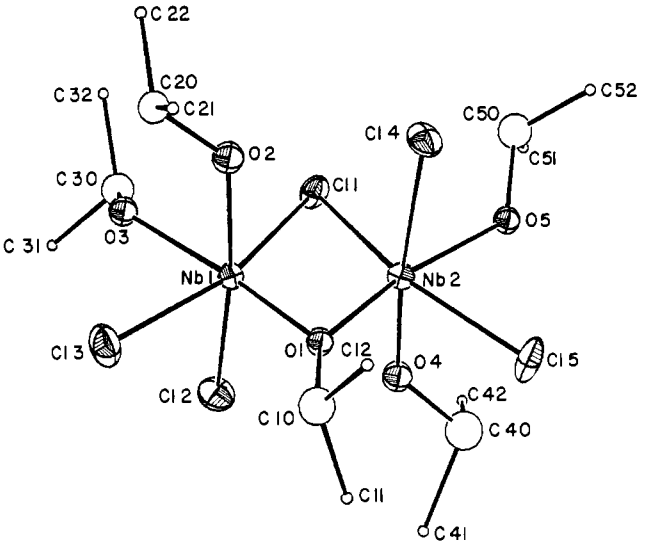

Figure 1. ORTEP view of the $Nb_2Cl_5(OPr)(HOPr)_4$ (**1c**) molecule. Methyl carbon atoms are drawn as arbitrarily small spheres for the sake of clarity.

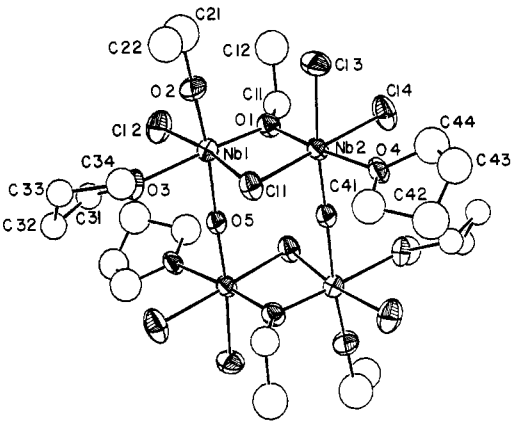

Figure 2. ORTEP view of the $[Nb_2OCl_4(OEt)_2(THF)_2]_2$ (**2b**) molecule. Only one orientation of the disordered THF and terminal ethoxide ligands is shown. Halves of the molecule are related by a center of symmetry.

the bridging atoms. The $Nb–O_{alcohol}$ lengths are strongly influenced by the trans ligand: those alcohol ligands trans to chlorine atoms are 0.14 Å closer to the metal than the alcohol ligands trans to the bridging propoxide group. The metal–chlorine distances are similarly influenced by the trans ligand, but less so: chlorine atoms trans to the bridging chlorine atom are about 0.05 Å closer to the metal atom than are those trans to an alcohol group.

Although hydrogen atoms were not located, the terminal ligands can be unambiguously assigned as alcohol rather than alkoxide groups on the basis of the following four criteria: First, the Nb–O distances are longer than those in compounds containing alkoxide ligands. Niobium to terminal alkoxide oxygen atom distances are typically near 1.8 Å.[7,11,13,15] Second, the Nb–O–C angles (131 [2]° in **1c**) are much more acute than those on terminal alkoxide ligands, which range from about 160 to near 180°. Third, in the proton NMR spectra of **1b** and **1c** there are peaks assignable to both axial and equatorial hydroxyl groups (vide infra). Finally, an O–H stretching band centered at 3200 cm^{-1} is seen in the IR spectra. The broadness of this band indicates the presence of hydrogen bonding, and no peaks due to an unhindered O–H stretch are seen. The orientation of the organic part of the alcohol groups suggests that intramolecular hydrogen bonding exists between O(2) and Cl(4), O(4) and Cl(2), O(3) and Cl(3), and O(5) and Cl(5). The atoms in these pairs are within hydrogen-bonding distances of one another; in each case the O···Cl distance is about 3 Å. On the basis of spectroscopic evidence, compounds **1a** and **1b** are presumed to have similar structures.

Compound **2b** exists as a centrosymmetric tetranuclear molecule in the solid state (see Figure 2). The tetramer consists of a pair of edge-sharing bioctahedra that are joined by two axial ligands. Considering for the moment only half of the tetramer, the similarity between the tetramer **2b** and dimeric **1b** becomes obvious. This is shown schematically, where groups lost from **1b** are circled:

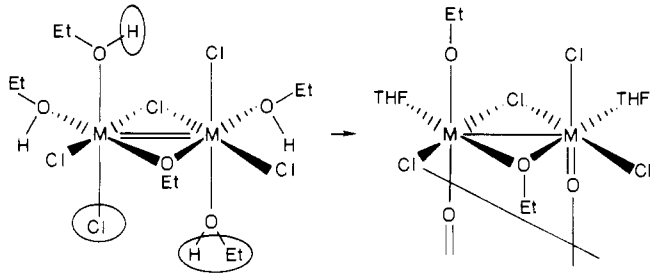

There is only a minor change in the equatorial plane, namely THF substitution of the ligating alcohol molecules. Two of the axial ligands also experience little or no change—one axial chlorine atom is retained and one alcohol molecule loses a proton to become an alkoxide. The second axial alcohol molecule is transformed to an oxo ligand with formal loss of a hydrogen atom and a C_2H_5 unit. The organic product of this reaction has been identified by GC–MS as C_2H_4; no evidence for C_2H_6 was seen. The second axial chlorine atom is replaced by an oxo ligand from another dimeric unit. The Nb–O–Nb bridge is not required to be either linear or symmetric. While the Nb–O–Nb angle does in fact approach linearity, there is a large difference in the Nb–O distances. This difference follows the trend outlined above, with the $Nb–O_{trans\ to\ Cl}$ distance about 0.20 Å shorter than the $Nb–O_{trans\ to\ O}$ distance.

Pairs of the d^1 metal atoms in **2b** participate in metal–metal bonding. Although the Nb(1)–Nb(2) distance, 2.891 (1) Å, is about 0.10 Å longer than most niobium–niobium single bonds, it is still much to short for a nonbonding interaction (cf. the Nb–Nb distance in Nb_2Cl_{10}, 3.951 Å). It is interesting to compare the metal–metal distances in **1c** and **2b**. The ligand sets in these compounds are similar, especially with regard to the bridging ligands. Yet in **1c** the metal–metal double bond is unusually short, about 0.1 Å shorter than most M=M double bonds (M = Nb, Ta), while the metal–metal single bond in **2b** is unusually long. One important difference between **1c** and **2b** is the lack of hydrogen bonding in **2b**. Hydrogen bonds in **1c** bridge the axial ligands, allowing them to come closer to one another than they can in **2b**. Repulsion between axial ligands has been assigned a significant role in the determination of metal–metal distances in edge-sharing bioctahedra.[19] Although other factors might be important here (e.g. replacement of a ROH and Cl ligand by two oxo ligands), a decrease in the axial ligand repulsions via hydrogen bond formation ought to significantly affect the ability of the metal atoms to approach one another.

Synthesis. $Nb_2Cl_6(THT)_3$ and $Ta_2Cl_6(THT)_3$ have long been recognized as versatile starting materials for compounds containing M–M double bonds. The two terminal THT ligands can readily be displaced by a number of other ligands to give compounds with face-sharing bioctahedral geometries.[20,21] Some ligands react further, resulting in rearrangement to an edge-sharing bioctahedral geometry with retention of the M–M double bond.[22] This is the case in the reaction of $Nb_2Cl_6(THT)_3$ with an excess of alcohol, where $Nb_2Cl_5(OR)(HOR)_4$ is initially formed in high yields. This diamagnetic compound can be isolated when R = Et or *i*-Pr. Although stable in the parent alcohol, solutions of $Nb_2Cl_5(OR)(HOR)_4$ (R = Et, *i*-Pr) in THF slowly decompose. Initially a soluble green compound forms. This green species then disappears, and a red compound forms with the concomitant liberation of a gas. When R = Et, the organic constituent of this gas was identified by GC–MS as ethylene. Presumably H_2 and HCl are the other products of the reaction. This reaction is completely reproducible under routinely maintained anaerobic conditions.

Although $Nb_2Cl_5(OMe)(HOMe)_4$ is initially produced when $Nb_2Cl_6(THT)_3$ reacts with methanol, it cannot be isolated in pure form because it decomposes upon workup. In toluene this decomposition leads to the formation of $Nb_2Cl_4(OMe)_4(HOMe)_2$.[15] This Nb(IV) dimer can also be made by the reaction of neat MeOH with $NbCl_4(THF)_2$[11] or $NbCl_4(CH_3CN)_3$,[12] and it crystallizes as the disolvate $Nb_2Cl_4(OMe)_4(HOMe)_2 \cdot 2MeOH$.[11]

Solution Behavior. Isolated $Nb_2Cl_5(OR)(HOR)_4$ (R = Et, *i*-Pr) dissolves readily in THF, initially forming a brown solution. The proton NMR spectra of both derivatives are complex and indicative of partial substitution of ROH by THF. In each case three Nb species are present: the unsubstituted dimer (I), a monosubstituted dimer (II), and a disubstituted dimer (III). Since the axial alcohol groups are bound more strongly to the metal than are the equatorial alcohol groups, as evidenced by the shorter $Nb–O_{axial}$ distances, it is probably the equatorial alcohol groups that are replaced by THF. This proposal is in accord with the crystal structure of $[Nb_2OCl_4(OEt)_2(THF)_2]_2$ (vide supra), in which the equatorial alcohol ligands are replaced by THF while the axial alcohol ligands have been transformed into alkoxide ligands.

The ^1H NMR spectrum of $Nb_2Cl_5(OEt)(HOEt)_4$ in THF-d_8 is shown in Figure 3. Peak positions and assignments are detailed in Table VI. Four multiplets are seen in both the methyl and methylene regions. They can be assigned to ethanol, bridging ethoxide, axial ethanol, and equatorial ethanol. Replacement of equatorial ethanol units by THF does not significantly alter the chemical shifts of the methyl and methylene protons on the remaining ligands. Thus only one signal is seen, for example, in the methyl region for the bridging OEt groups of all three species. Peak assignments in the methyl and methylene regions are based on decoupling experiments and on the spectrum obtained after addition of a small amount of EtOH to the solution.

The region of the hydroxyl protons is more complicated. Five peaks are seen: four triplets (between 9.0 and 9.5 ppm) and a complex multiplet (near 8.0 ppm). Selective decoupling experiments indicate that all four of the downfield peaks are coupled to the methylene protons on the axial alcohol ligands. Irradiation of the equatorial methylene protons results in a collapse of the multiplet at 8 ppm to two peaks of unequal intensity. Of these two peaks, the more intense downfield one is assigned to the hydroxyl proton of the lone equatorial alcohol ligand in the monosubstituted compound, II. The other peak is assigned to the two equatorial alcohol groups in the unsubstituted compound, I.

Table VI. Proton NMR Peak Positions and Assignments for $Nb_2Cl_5(OEt)(HOEt)_4$ in THF-d_8

peak[a]	*J*[b]	assignt[c]	
9.41	5	ax. IIA	hydroxyl region
9.29	5	ax. I	
9.19	5	ax. III	
9.06	5	ax. IIB	
8.03	6	eq I	
7.97	6	eq II	
5.90		bridge	methylene region
4.31		ax.	
4.00		eq	
3.52		free EtOH	
1.45	7	ax.	methyl region
1.35	7	bridge	
1.23	7	eq	
1.11	7	free EtOH	

[a] Peak positions reported in ppm relative to $(CH_3)_4Si$. [b] Coupling, in Hz, to the methylene protons. [c] There are two types of axial ethanol ligands in II. "A" refers to those attached to the unsubstituted metal atoms, and "B" refers to those attached to the metal atom to which a THF molecule is bound. Abbreviations: ax., axial; eq, equatorial.

(19) Shaik, S.; Hoffmann, R.; Fisel, C. R.; Summerville, R. H. *J. Am. Chem. Soc.* **1980**, *102*, 4555.
(20) Cotton, F. A.; Duraj, S. A.; Roth, W. J. *Acta Crystallogr., Sect. C: Cryst. Struct. Commun.* **1985**, *C41*, 878.
(21) Cotton, F. A.; Diebold, M. P.; Kriechbaum, G.; Meadows, J.; Roth, W. J., unpublished results.
(22) Cotton, F. A.; Roth W. J. *Inorg. Chem.* **1983**, *22*, 3654 and references therein.

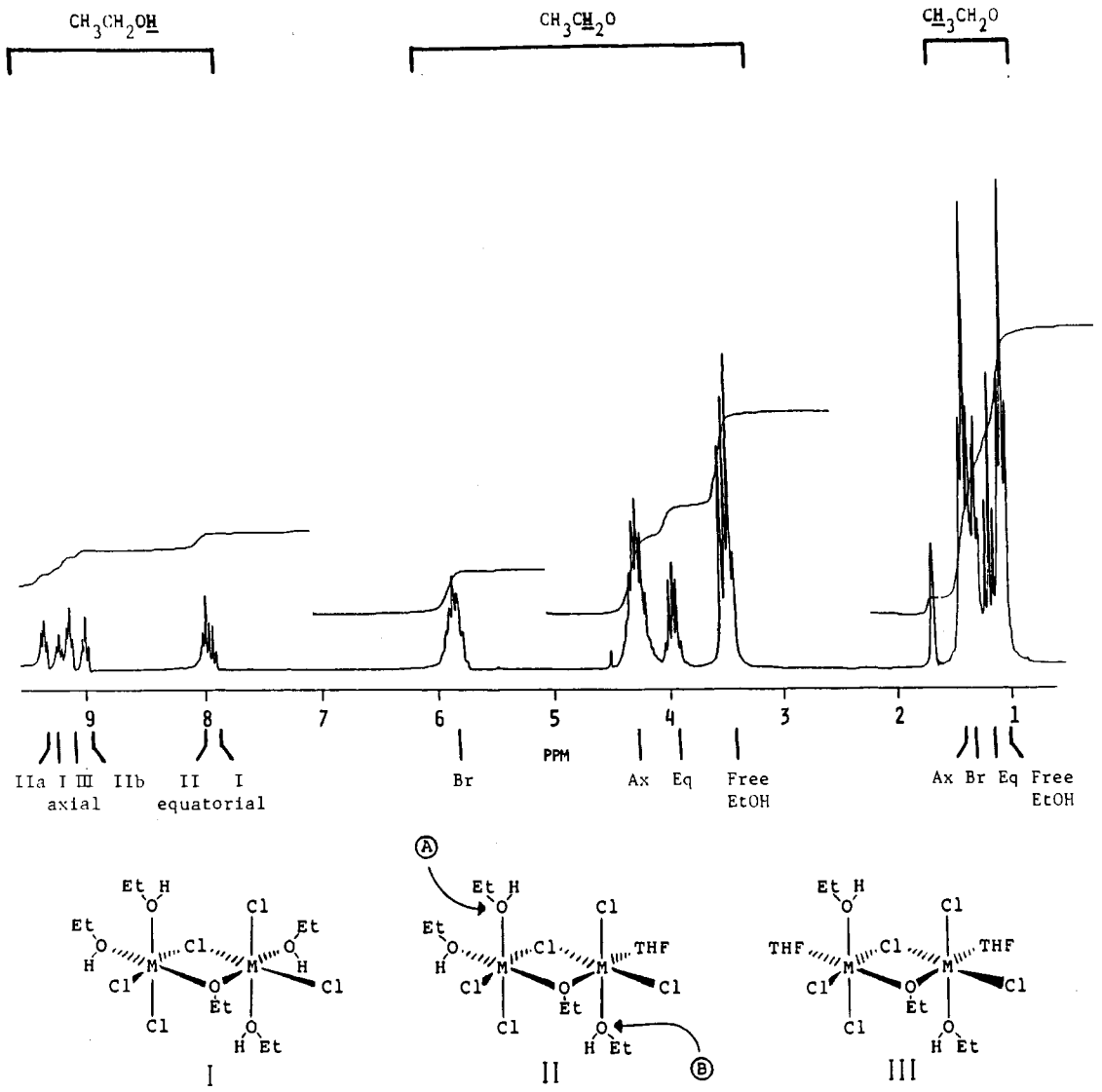

Figure 3. Proton NMR spectrum, with assignments, of $Nb_2Cl_5(OEt)(HOEt)_4$ (**1b**) in deuteriated THF.

From the relative areas of these peaks the ratio of concentrations of I:II can be determined and is used in the assignment of the axial hydroxyl peaks. It should be noted that reversing the assignments of the equatorial hydroxyl peaks leads to a calculated ratio of concentrations of I:II that is not consistent with the intensities of the axial hydroxyl peaks. In II the axial alcohol ligands are not equivalent, and the two axial hydroxyl peaks of equal intensity are assigned to these two different types of axial ligands. From the ratio of I:II calculated above, the peak at 9.29 ppm can be assigned to I and, by process of elimination, the remaining peak, at 9.19 ppm, is assigned to III. Of the two axial hydroxyl peaks in II, the upfield one, at 9.06 ppm, is assigned to the ligand attached to the metal on which substitution had occurred. This assignment is based on the proximity of this peak to that of the hydroxyl proton in III.

The relative areas of the hydroxyl proton peaks do not change with time, indicating that the three species are in equilibrium. However, over time the combined area of these peaks decreases, with a concomitant appearance of peaks near 10 ppm. THF solutions of **1b** and **1c** slowly turn green and then red as bubbles of gas form. Isolation and crystallization of the red complex has led to its identification as $[Nb_2OCl_4(OR)_2(THF)_2]_2$. This spontaneous transformation occurs with oxidation of the metals to the +4 state. Compound **1a** also is unstable with respect to oxidation, but in this case the end product is $Nb_2Cl_4(OR)_4(HOR)_2$. The reason the methoxide complex decomposes by a different route than the ethoxide and 2-propoxide cannot be stated with certainty, but it probably has to do with the higher acidity of methanol and with a lack of organic products that can be eliminated.

Acknowledgment. We are grateful to the National Science Foundation for support. M.P.D. thanks the National Science Foundation for a NSF Predoctoral Fellowship and Texaco/IUCCP for additional support.

Supplementary Material Available: For the crystal structures of **1c** and **2b**, complete listings of bond distances and angles and tables of anisotropic displacement parameters (6 pages); for both structures, tables of observed and calculated structure factors (13 pages). Ordering information is given on any current masthead page.